Human Molecular Genetics, 2007, Vol. 16, No. 7 ***731–741***
doi:10.1093/hmg/ddm028
Advance Access published on March 1, 2007

COG8 deficiency causes new congenital disorder of glycosylation type IIh

Christian Kranz[1,†], Bobby G. Ng[1,†], Liangwu Sun[1], Vandana Sharma[1], Erik A. Eklund[1,‡], Yoshiaki Miura[1,¶], Daniel Ungar[2], Vladimir Lupashin[3], R. Dennis Winkel[4], John F. Cipollo[5], Catherine E. Costello[5], Eva Loh[6], Wanjin Hong[6] and Hudson H. Freeze[1,*]

[1]Burnham Institute for Medical Research, La Jolla, CA 92037, USA, [2]Princeton University, Department of Molecular Biology, Princeton, NJ 08544, USA, [3]University of Arkansas for Medical Sciences, Little Rock, AR 72205, USA, [4]Highland Park Professional Building, Kalispell, MT 59901, USA, [5]Boston University School of Medicine, Boston, MA 02118-2526, USA and [6]Institute of Molecular & Cell Biology, 61 Biopolis Drive, Singapore 138671, Singapore

Received February 9, 2007; Revised and Accepted February 12, 2007

We describe a new Type II congenital disorder of glycosylation (CDG-II) caused by mutations in the conserved oligomeric Golgi (COG) complex gene, *COG8*. The patient has severe psychomotor retardation, seizures, failure to thrive and intolerance to wheat and dairy products. Analysis of serum transferrin and total serum *N*-glycans showed normal addition of one sialic acid, but severe deficiency in subsequent sialylation of mostly normal *N*-glycans. Patient fibroblasts were deficient in sialylation of both *N*- and *O*-glycans, and also showed slower brefeldin A (BFA)-induced disruption of the Golgi matrix, reminiscent of COG7-deficient cells. Patient fibroblasts completely lacked COG8 protein and had reduced levels and/or mislocalization of several other COG proteins. The patient had two COG8 mutations which severely truncated the protein and destabilized the COG complex. The first, IVS3 + 1G > A, altered the conserved splicing site of intron 3, and the second deleted two nucleotides (1687–1688 del TT) in exon 5, truncating the last 47 amino acids. Lentiviral-mediated complementation with normal COG8 corrected mislocalization of other COG proteins, normalized sialylation and restored normal BFA-induced Golgi disruption. We propose to call this new disorder CDG-IIh or CDG-II/COG8.

INTRODUCTION

The conserved oligomeric Golgi (COG) complex is an eight subunit (COG1–8) peripheral Golgi membrane hetero-oligomeric protein complex (1,2). The COG complex is organized into lobes A (COG2–4) and B (COG5–7) with COG1 and COG8 bridging these lobes (3,4). The COG complex is thought to play a critical role in vesicle tethering processes involving retrograde Golgi transport (5–8) of resident proteins responsible for sugar chain (glycan) biosynthesis.

Since proper glycosylation relies not only on the presence of the biosynthetic enzymes but also on their appropriate distribution and localization within the Golgi, COG deficiencies are thought to disturb this highly organized and finely tuned trafficking of glycosyltranferases, nucleotide sugar transporters and glycosidases. This explains why COG disruption causes glycosylation defects in various pathways.

COG functions are essential and mutants deficient for COG proteins have been found in various organisms. Chinese hamster ovary cell mutants, ldlB and ldlC, carry mutations in COG1 and COG2, respectively, and both display pleiotropic defects in *N*-linked glycan, *O*-linked glycan and glycosphingolipid synthesis (9). Mutants for each COG subunit were identified in *Saccharomyces cerevisiae* (10–14). The subunits Sec34/Sec35 corresponding to COG3 and COG2 were identified first (13,14). Complete knockout of COG subunits in

*To whom correspondence should be addressed at: Glycobiology and Carbohydrate Chemistry Program, Burnham Institute for Medical Research, 10901 N. Torrey Pines Rd, La Jolla, CA92037, USA. Tel: +1 8586463142; Fax: +1 8587136281; Email: hudson@burnham.org
†These authors contributed equally.
‡Present address: Lund University, Department for Cell and Molecular Biology, BMC C13, 221 84 Lund, Sweden.
¶Present address: Hokkaido University, Sapporo, Japan.

yeast leads to variable phenotypes ranging from lethality (COG4) to minor deficiencies observable as oligosaccharide maturation defects (COG8).

A COG5 deficiency in *Drosophila melanogaster* produces viable flies, but males are sterile because of incomplete spermatogenesis (15). COG1 and COG3 mutants of *Caenorhabditis elegans* exhibit problems with gonadal distal tip cell (DTC) migration. The underglycosylation of MIG-17, a metalloprotease involved in the control of DTC migration, leads to its mislocalization and ultimately causes abnormal gonadal shape (16).

Recently, two human disorders were identified as being caused by mutations in *COG7* (17) and *COG1* (18). The COG7-deficient patients died in early infancy and the COG1-deficient patient suffers from psychomotor retardation and hypotonia. Both disorders are members of a rare group of inherited metabolic disorders named congenital disorders of glycosylation (CDG). Cells from COG7- and COG1-deficient patients exhibit multiple glycosylation abnormalities caused by reduced glycosyltransferase activities and nucleotide sugar transport. Direct measurement of GFP-tagged sialyltransferase (ST3Gal1) using Fluorescence Recovery After Photobleaching (FRAP) shows that the repopulation of the bleached Golgi is 2–3 times slower than in control cells (17). Similar conclusions were derived from the rate of brefeldin A (BFA)-induced Golgi disassembly. COG7-deficient fibroblasts treated with BFA revealed that COG7 plays an important role in efficient Golgi-to-ER retrograde transport (19). Measuring the rate of BFA-induced Golgi disruption is technically simpler than GFP-FRAP, but it is unknown whether other COG deficiencies alter the effects of BFA on Golgi dissociation.

CDG patients are divided into two groups, referred to as CDG-I and CDG-II, on the basis of the identity of the defective gene. All defects that alter the synthesis of the lipid-linked oligosaccharide ($Glc_3Man_9GlcNAc_2$) or its transfer to protein are assigned to the first group (CDG-I), whereas defects that affect the processing of the protein-bound oligosaccharide are within the second category (CDG-II) (20,21). Both COG deficiencies are members of the second group.

In this paper, we describe the first patient with a COG8 deficiency due to two heterozygous mutations in the human *COG8* gene. We propose to call this CDG-IIh or CDG-II/COG8. Both mutations truncate the COG8 protein, which is degraded, and this in turn mislocalizes and/or destabilizes selected subunits of the COG complex especially those in lobe B. Abnormal *N*- and *O*-glycosylation could be detected in patient's fibroblasts while abnormal *N*-glycosylation could be shown in serum. Clinical consequences of the COG8 deficiency are severe psychomotor retardation and hypotonia.

RESULTS

Clinical phenotype

The patient had a normal birth at term. His prenatal ultrasound, birth weight (2950 grams) and physical examination were normal. Nothing unusual was noted except for excessive crying, gas and bloating, which occurred during the first 6–7 months. However, by 7 months, the patient was recognized to be hypotonic with poor head control and he did not reach for objects. It was noted that at this age he did not sit or roll over. His reflexes were decreased.

Karyotype was normal and skin biopsy excluded lysosomal storage disorders. Lactate was slightly elevated. Nerve biopsy showed chronic axonal neuropathy and a muscle biopsy showed a neurogenic process, but no evidence of a mitochondrial disorder. Further evaluation by MRI showed ventriculomegali *ex vacuo* with atrophy, and sonar spectroscopy revealed high levels of lactate in the gray matter.

The initial electroencephalograms were essentially normal, but he subsequently developed myoclonic jerks at 18–24 months with electroencephalographic slow waves consistent with seizures. The patient responded poorly to lamotrigine. His esotropia/amblyopia was treated with eye patching.

At 8.5 years, he is severely retarded with no speech, nor any bowel or bladder control. He follows well with his eyes. Intolerance to wheat and dairy products causes abdominal pain and bloating, but he is relatively healthy. Both height (95 cm) and weight (10.9 kg) are below the first percentile. He presents striking lack of muscle from all areas, resembling severe malnutrition. He has dry skin with *keratosis pilaris*. There is mild spastic posturing of both hands and mild contractures of the lower extremities.

Analysis of *N*- and *O*-glycosylation

These clinical features were within the CDG spectrum, and serum transferrin was analysed by ESI-MS to determine abnormal glycosylation. Figure 1A shows that a substantial portion of patient's transferrin is missing one (Δ291 Da) and a very small amount missing two sialic acid residues (Δ582 Da). To determine whether the observed sialylation deficiency is restricted to transferrin alone or affects other glycoproteins as well, *N*-glycans were released from total serum proteins by PNGase F digestion and labelled with 2-aminobenzamide. Separation by anion-exchange HPLC showed a substantial decrease in the proportion of glycans with ≥ 2 sialic acids and a corresponding increase in glycans with only one sialic acid in comparison with control (Fig. 1B). There was no increase in the amount or general pattern of neutral glycans (see inset Fig. 1B) showing that at least one sialic acid could be added to chains which normally have 2–4 sialic acids. The increase in one charged material was confirmed by MALDI-TOF analysis of total serum *N*-glycans. The amount of biantennary glycans lacking one galactose and one sialic acid was slightly increased compared with control confirming that a sialylation, rather than a galactosylation, deficiency caused the increase in single charged material. The MALDI-MS spectrum of the neutral glycans from patient and control serum showed slightly increased fucosylated agalacto-asialo glycans, but that small difference cannot account for the major increase of hyposialylated material (data not shown).

Patient and control serum derived $Sial_1Gal_2Man_3GlcNAc_4$ were analyzed to determine whether the sialic acid is added to the antenna build on the alpha-1,3-linked or the alpha-1,6-linked mannose residue. The collision-induced dissociation (CID) mass spectrum of standard $Sial_1Gal_2Man_3GlcNAc_4$ containing both isomers is shown in Figure 1C.1. The CID spectrum shows D_{4-5} fragments from both isomers. The isomer

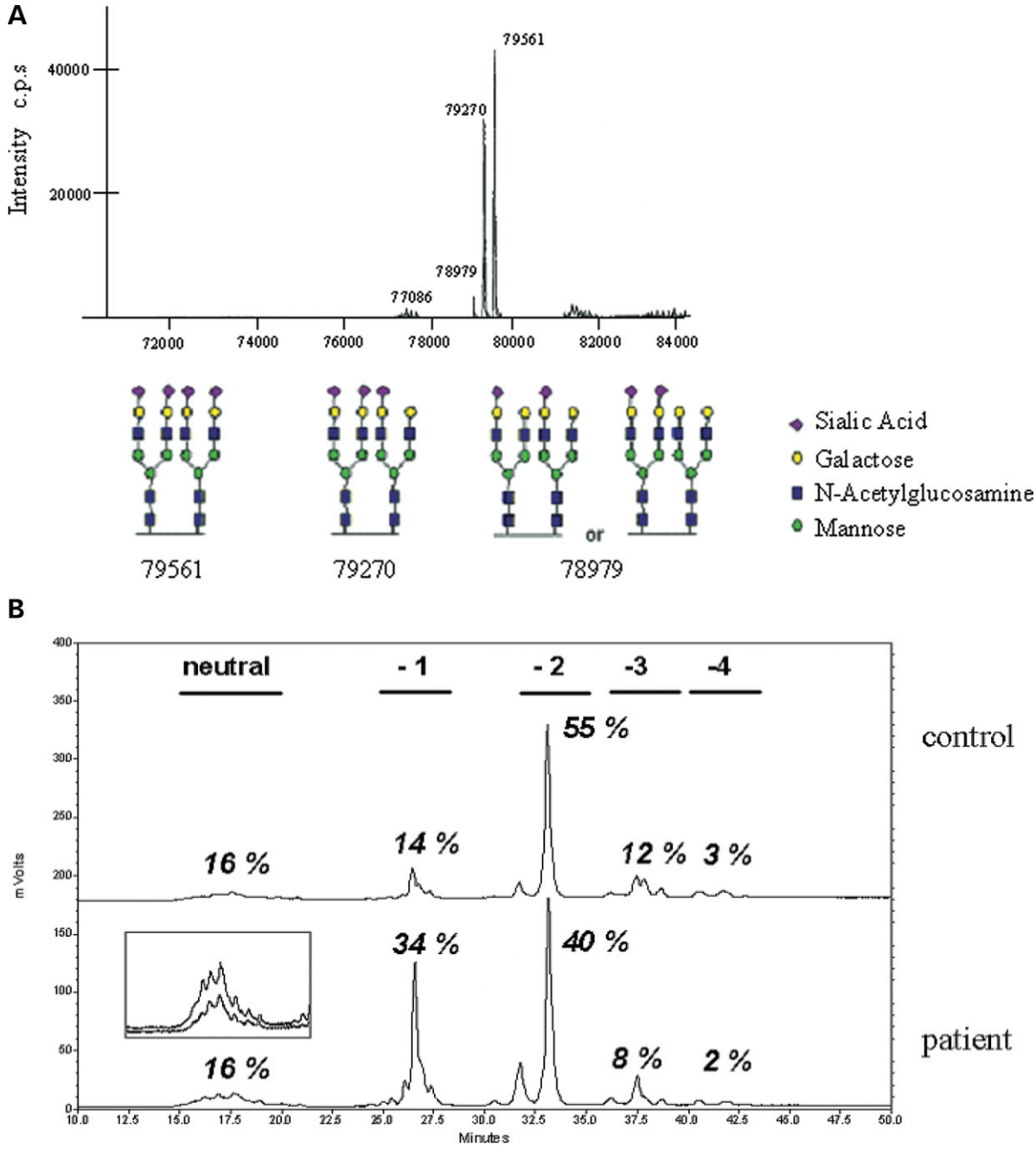

Figure 1. Analysis of transferrin, serum *N*-glycans, and fibroblast *O*-glycans. ESI-MS of serum transferrin and structural analysis of serum *N*-glycans. (**A**) ESI-MS spectrum of immunopurified serum transferrin. Fully sialylated normal Tf has a mass of 79561, but the loss of one sialic acid (mass 291) generates a glycoform of 79270. Loss of two sialic acids (2 × 291) generates a form of mass 78979. The undersialylated forms are not seen in controls. (**B**) PNGase F-released oligosaccharides from patients and control sera were labeled with 2-aminobenzamide and separated by anion exchange HPLC. The numbers over the bars indicate the charge of the glycans. The increase in singly charged glycans in the patient shows loss of only a single Sia, but no increase in neutral *N*-glycans as shown in the insert. Neutral glycan distributions are similar in patient and control serum. See text for details. (**C**) Negative ion CID mass spectra of biantennary monosialylated glycans. The CID spectrum of a $Sia_1Gal_2Man_3GlcNAc_4$ standard containing sialic acid on the α1,6-branch or the α 1,3-branch is shown in 1. The CID spectra of $Sia_1Gal_2Man_3GlcNAc_4$ derived from normal and patient serum are shown in 2 and 3, respectively. The structures and key fragment ions of both isomers are shown above the spectra. Biantennary glycans of both patient and control contain Sia primarily on the α 1,3-linked arm. (**D**) Amine adsorption HPLC analysis of [^{3}H]Gal labeled GAP products (*O*-linked glycosides) synthesized and secreted by control (open circles) and patient cells (filled circles). The cells were labeled with 250 μM GAP and the labeled product was secreted into the medium which was bound and eluted from C18 SepPak cartridge and analyzed by HPLC as described in Kim *et al*., 2001 (23). Molecular structures above each peak represent glycans eluted in those fractions (∀ GalNAc, ν GlcNAc, λ Gal and υ Sialic acid). The numbers above the glycans indicate the % radioactivity in the peak with patient in bold font.

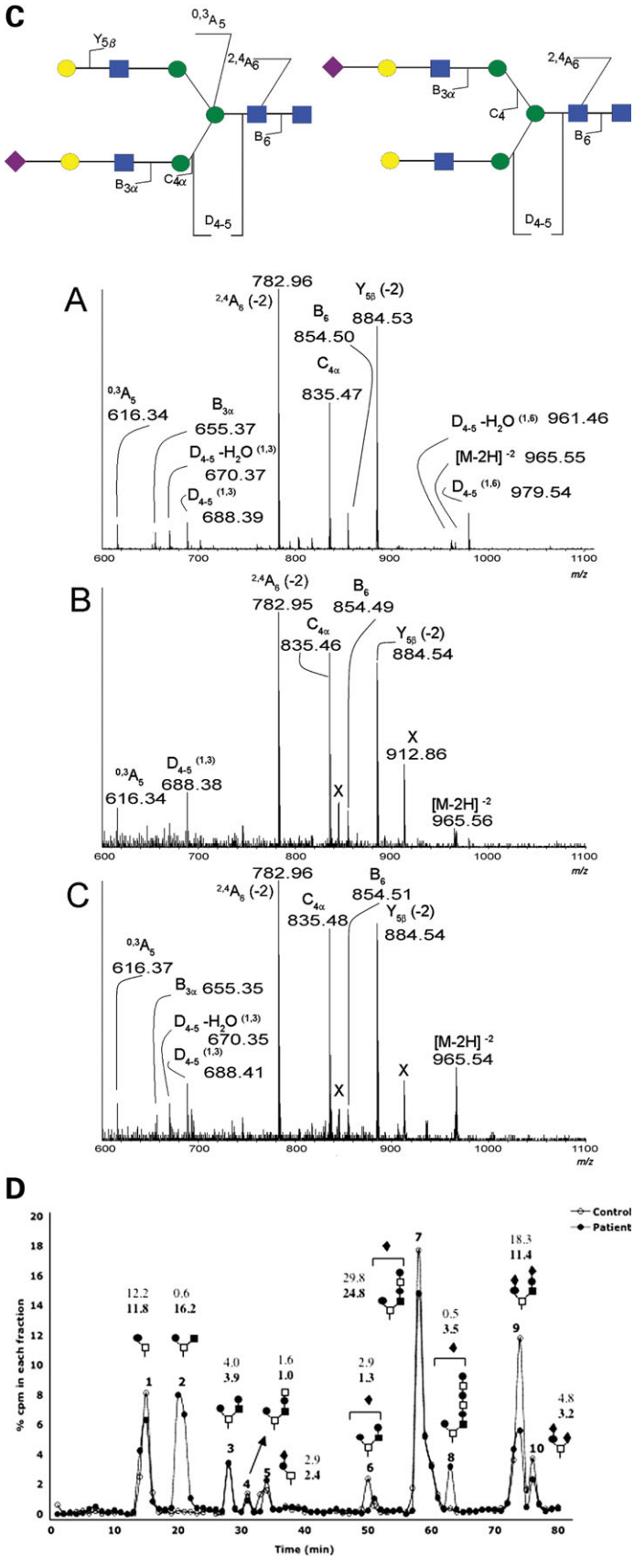

Figure 1. Continued

Table 1. Galactosyl- and sialyltransferase activities of control and patient cells

Enzyme	Control (pmol/min/mg)	Patient (pmol/min/mg)
beta-1,3-GalT, (%)	107 ± 0.7 (100)	96 ± 4.9 (90)
beta-1,4-GalT, (%)	359 ± 17.6 (100)	284 ± 15.5 (80)
ST3GalI, (%)	1.9 ± 0.049 (100)	0.69 ± 0.057 (36)
ST3GalIII, (%)	98 ± 3.2 (100)	96 ± 2.4 (98)

Numbers in brackets show relative activities. Values represent the mean of three independent experiments.

with the 1,6-branch sialic acid produces D_{4-5} and $D_{4-5}-H_2O$ ions at *m/z* 979.54 and 961.46 respectively. The isomer with the 1,3-branch sialic acid produces D_{4-5} and $D_{4-5}-H_2O$ fragment ions at *m/z* 688.39 and 670.37. The 1,3-branch sialic acid isomer also produces an $^{0,3}A_5$ fragment was observed at *m/z* 616.34. All of these ions are unique to the respective isomers. The CID spectrum from control serum-derived $Sial_1Gal_2Man_3GlcNAc_4$ is shown in Figure 1C.2. The D_{4-5} and $^{0,3}A_5$ fragment ions were observed at *m/z* 688.41 and 616.37, respectively. Only a trace amount of D_{4-5} fragment ions were observed at *m/z* 979.55 and 961.46 showing that the predominant isomer in the normal control serum has sialic acid on the 1,3-branch. The corresponding CID spectrum from the patient (Fig. 1C.3) shows the D_{4-5} and $^{0,3}A_5$ ions specific to the 1,3-branch-linked sialic acid. These data demonstrate that the patients monosialated $Sial_1Gal_2Man_3GlcNAc_4$ serum-derived glycan contains sialic acid predominantly on the 1,3-linked branch.

Serum *N*-glycans primarily contain alpha-2,6 sialic acid. The activities of both sialyltransferases (ST6GalI and ST6GalTII) that carry out the alpha-2,6-sialylation of *N*-glycans were not measurable in fibroblasts, but sequencing of their corresponding exons and splice sites of genomic DNA found no mutations.

Finding sialylation-deficient serum *N*-glycans led to the investigation of patient fibroblasts metabolically labeled with [^{3}H]-mannose. PNGase F-released *N*-glycans were analyzed by QAE-Sephadex ion-exchange chromatography and showed an increase in the one charged material (9.5 versus 14% of total) and in neutral glycans (61 versus 70%) in control and patient cells, respectively. Radioactivity in the fractions representing the two, three and four charged material decreased accordingly (no figure shown). Concanavalin A lectin affinity chromatography of the same material showed no differences between patient and control demonstrating normal branching of patient's *N*-glycans (data not shown).

A possible explanation for the reduced sialylation could be reduced transport of CMP-sialic acid into the lumen of the Golgi, but it was found to be normal in patient fibroblasts compared with control (data not shown). UDP-galactose transport into the Golgi was also normal. Fibroblasts primarily synthesize alpha-2,3-linked sialic acid on *N*-glycans. The activity of the relevant sialyltransferase (ST3GalIII) from the patient was, however, normal (Table 1).

In contrast, ST3GalI activity that adds alpha-2,3 sialic acid to Core1 *O*-linked glycans showed a decrease of 64% compared with control (Table 1). Reduced ST3GalI activity suggested that sialylation of *O*-glycans might also be compromised. To test this, we used fluorescently tagged Peanut Agglutinin (PNA) which binds to non-sialylated Core1 *O*-glycans (Galβ1,3GalNAc) (22). As can be seen in Figure 5B, control fibroblasts have almost no detectable PNA staining, since terminal sialic acid residues block binding to the lectin. In contrast, patient's cells show a much brighter staining indicating the incomplete addition of terminal sialic acid residues to fibroblast *O*-glycans. Sialidase digestion exposes the penultimate galactose residues, and produces equivalent PNA staining of control and patient fibroblasts. To confirm that the patient had altered *O*-glycans, cells were incubated with GalNAcα-phenyl (GAP), which is an alternate acceptor for *O*-GalNAc-linked glycans, and reflects the cell's synthetic capacity (23). HPLC analysis of secreted [6^{3}H]galactose-labeled GAP-glycans (Fig. 1D) shows that the patient has a 2-fold increase in non-sialylated species and decreased disialylated species. This result is consistent with the PNA binding difference and the lower ST3Gal1 activity in the patient cells (Table 1). Both control and the patient synthesize the same proportion of branched Core2 structures (∼62%).

Activities of galactosyltransferases responsible for the beta-1,4 galactosylation of *N*-glycans and the beta-1,3 galactosylation of *O*-glycans were within the normal range (Table 1).

These results demonstrate that the sialylation of both *N*- and *O*-glycans is affected in the patient cells, a phenomenon that has previously been described in cells from COG-deficient patients (CDG-IIe and CDG-IIg).

BFA-induced retrograde transport

Steet and Kornfeld (19) showed that COG7-deficient fibroblasts have a significant delay in retrograde transport of the Golgi matrix protein giantin into the ER. Moreover, a portion of COG7-deficient fibroblasts retained a cluster of giantin in juxtanuclear position even after prolonged exposure to BFA. This cluster co-localizes with the microtubule-organizing center (MTOC) as shown by its co-localization with γ-tubulin (19). The MTOC organizes pre-Golgi intermediates before they are transported to the Golgi. COG deficiencies are thought to prevent those intermediates from exiting the centromere in the presence of BFA.

To test if fibroblasts obtained from the patient also show slower kinetics of retrograde transport, cells were incubated with medium containing 0.25 μg/ml BFA. The localization of giantin was observed after different times in fixed cells. Figure 2A shows that transport in the patient's fibroblasts is significantly slower than in control cells. Similar to COG7-deficient cells, a giantin cluster in juxtanuclear position remains in about 30–40% of patient's fibroblasts after prolonged exposure to BFA. These clusters also co-localize with γ-tubulin indicating its close proximity to the MTOC (Fig. 2B). These clusters do not occur in control cells (<2%).

Western blotting and immunofluorescence of COG and GEAR proteins

Since the BFA-induced retrograde transport was similar to COG7-deficient patient fibroblasts, Western Blot analysis was performed for all COG subunits. As shown in

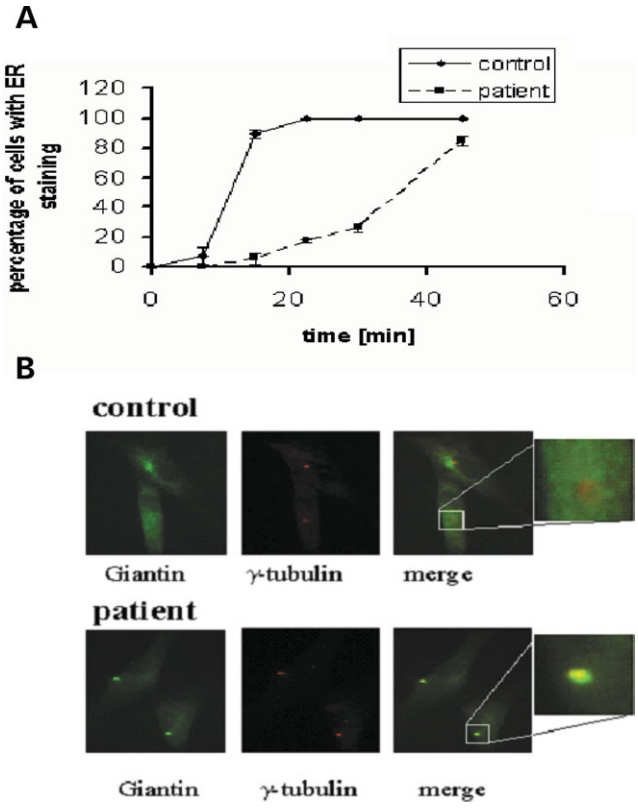

Figure 2. BFA-induced retrograde transport kinetics of control and patient cells. (**A**) Control and patient fibroblasts were treated with 0.25 μg/ml BFA. Cells have been fixed as described at different time points and the localization of the Golgi matrix protein giantin was observed by immunofluorescence using an Alexa-488 coupled anti giantin antibody. The percentage of cells without Golgi staining were shown at the given time points. Between 50 and 100 cells were counted in replicate samples for each time point. (**B**) Double staining of giantin and γ-tubulin after 60 min incubation with 0.25 μg BFA. Golgi juxtanuclear cluster were observable in 30–40% of the patient's cells and co-localize with γ-tubulin. No co-localization was observable in control cells.

Figure 3A, the most noticeable difference between patient and control blots was the complete absence of COG8. Moreover, COG1, COG5, COG6 and COG7 were also reduced but there was no reduction in COG2, COG3 and COG4. Immunofluorescence (Fig. 3B) shows that COG8 was absent from patient cells and COG5, COG6 and COG7 were mislocalized compared with control.

A subset of Golgi proteins, the so-called GEAR proteins GS15 and GPP130, are decreased in various Cog-deficient cells (24). Western blot analysis (Fig. 3A) shows they are also decreased in patient's cells.

Sequencing of the *COG8* gene

Since detectable COG8 protein was completely missing as determined by western-blotting and immunofluorescence, the corresponding gene (NM_032382) was sequenced. The patient is compound heterozygous for two mutations. (Fig. 4) The first mutation (IVS3 + 1G > A) alters the donor splice site of exon 3 by converting the highly conserved GT donor splice site sequence to AT. cDNA sequencing revealed an alternate splice site in the middle of exon 3 is used instead, leading to the splicing of the first 913 bp of the *COG8* gene (containing exon 1, exon 2 and 327 bp of exon 3) to exon 4. The alternative splicing truncates the *COG8* mRNA by 500 bp and the resulting frame shift produces a termination codon directly after the spliced-out sequence, and ultimately shortens the protein by 306 C-terminal amino acids.

The second mutation deletes two base pairs from the coding sequence (1687–1688 del TT) and the resulting frame shift induces a premature stop codon after three missense amino acids. This truncates the protein by 47 C-terminal amino acids. Both parents were heterozygous for one of the mutations. All other COGs were sequenced, but no additional mutations were found.

Lentiviral complementation of patient cells

To verify the functional importance of the mutations found in the *COG8* gene of the patient, a wild-type copy of the respective gene was transduced into the patient fibroblasts using a lentiviral delivery system. Cells were monitored for various parameters, 4–5 days after transduction. As can be seen in Figure 5C, the complementation with the wild-type *COG8* gene almost completely restored the retrograde transport kinetics observed by intracellular giantin distribution of patient cells. In addition to this, COG5, COG6 and COG7 regained a normal Golgi distribution (Fig. 5A) and PNA staining returned to normal after the wild-type gene was delivered (Fig. 5B).

DISCUSSION

This paper describes the discovery of the first patient suffering from CDG-IIh, a disease caused by mutations in the *COG8* gene. Sequencing of the *COG8* cDNA revealed two mutations that ultimately lead to a truncated and apparently unstable COG8 protein. The complementation of patient's fibroblasts with the wild-type *COG8* gene proved the functional importance of the mutations.

The key to the analysis of the COG subunits was an assay introduced by Steet and Kornfeld (19), who showed that COG7-deficient fibroblasts have a much slower transport of Golgi proteins to the ER in response to BFA treatment. BFA leads to a rapid release of COPI and AP-1 from Golgi membranes into the cytosol resulting in the formation of tubules emanating from the Golgi (19,25,26). When those tubules fuse with the ER membranes, it causes a rapid collapse of the Golgi into the endoplasmic reticulum. Fibroblasts derived from our patient exhibited significantly slower transport kinetics than control, similar to that seen in COG7-deficient patients. It is likely that this simple method can be applied to test cells from other potential COG-deficient patients. While it may not be a specific test for a defective COG complex, it may be a way to implicate other trafficking defects between Golgi and ER.

Further characterization of the COG complex proteins by western blotting and immunofluorescence revealed that the amounts of COG1, COG5, COG6 and COG7 were reduced and COG8 was almost completely absent. Since no truncated COG8 protein appeared on the western blots, it seems most

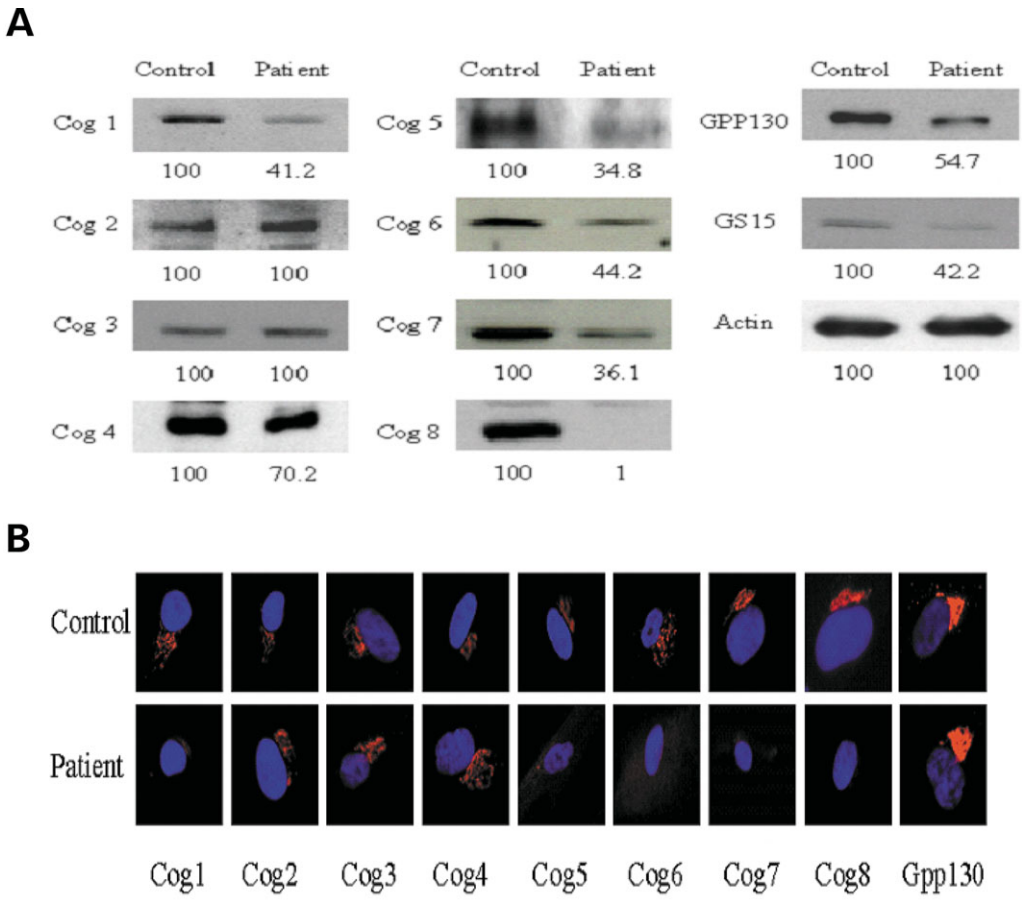

Figure 3. Western blot analysis and immunofluorescence of Cog subunit distribution in control and patient fibroblasts. (**A**) Western blots of COG subunits, actin, GS15 and GPP130. Samples were normalized to actin and quantified using Scion Imaging. The percentages given are the amount remaining compared with control. (**B**) Immunofluorescence of all COG subunits in patient and control fibroblasts. Fixed cells were stained with COG 1–8 as well as Golgi specific markers GPP130 or GM130. In the case of patient cells, very little to no Golgi staining was seen for COG5–8 compared with control fibroblasts.

likely that the mutated protein variants are highly unstable, rather than loss of specific epitopes recognized by the polyclonal antibody. Moreover, all subunits of lobe B were mislocalized. These findings are in good agreement with the current model of the proposed architecture of the COG complex (3,4,27). Lobe A consists of COG2, COG3 and COG4 and lobe B contains COG5, COG6 and COG 7 and the two lobes are bridged by COG1 and COG8 (3,4). According to this model, the absence of COG8 would prevent direct binding to COG1 and destabilize all subunits of lobe B.

The patient described in this study showed abnormal *N*- and *O*-glycosylation as shown by ESI-MS analysis of serum transferrin and PNA staining of affected fibroblasts. The detailed structural analysis of serum *N*-linked glycans revealed a dramatic increase in monosialylated glycans with a corresponding decrease in species with 2–4 sialic acids. Since only small changes occurred in the amount or composition of the neutral glycans, we conclude that the major effect on glycosylation is the addition of the second sialic acid to otherwise generally normal *N*-glycans. Both, ESI-MS analysis of serum transferrin and the detailed analysis of total serum *N*-glycans revealed quite substantial absence of single sialic acid residues, especially on biantennary *N*-glycans, the most prevalent glycan on serum glycoproteins. The incomplete addition of sialic acid to biantennary *N*-glycans preferentially affects the branch built on alpha-1,6-linked mannose of the glycan core.

In addition, *O*-glycan biosynthesis using the alternate acceptor substrate, GAP, in conjunction with PNA lectin staining shows that patient did not sialylate these glycans as well as control. This may result from the patient's lower ST3Gal1 activity or be due to altered distribution or trafficking of the enzyme through the Golgi. We cannot distinguish between these alternatives.

More extensively, misglycosylated structures, including abnormally galactosylated glycans, are seen in samples from other CDG-II patients (18,28–30). The finding of a sialylation deficiency leading to the large accumulation of monosialylated biantennary chains in both transferrin and total serum *N*-glycans, is novel. Reduced sialylation of *O*-glycans was also seen, without any effect on the proportion of Core1 and Core2 structures. CMP-sialic acid transport into the Golgi and ST3GalIII activity were normal in patient fibroblasts, and no mutations were found in ST6GalI or ST6GalII.

In contrast to COG7-deficient fibroblasts, COG8 cells do not have major galactosylation deficiencies or exhibit problems in the transport of nucleotide-sugars into the

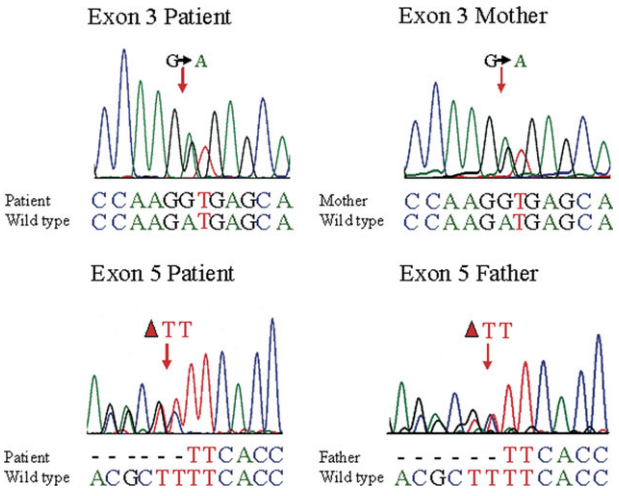

Figure 4. Sequence analysis of Cog8. Sequence analysis from mother and father as well as patient's genomic DNA revealed two mutations. The first, IVS3 + 1G > A, altered the conserved splicing site of Intron 3, and the second deleted two nucleotides (1687–1688 del TT) in Exon 5, truncating the last 47 amino acids.

lumen of the Golgi. The COG8 deficiency seems to mainly affect sialylation. It is possible that the COG8 deficiency rather specifically decreases the time hepatocyte-derived glycoproteins co-reside with sufficient ST6GalI/II and CMP-sialic acid transporter-delivered substrate. Ultimately, the abbreviated residence time leads to undersialylated *N*- and *O*-glycans. The reason for absence of sialic acid from the alpha-1,6-mannose linked branch of biantennary glycans is probably that its addition is 10–40 times slower than the addition of sialic acid to the alpha-1,3 branch (31–33). Against this kinetic background, a shorter co-residence time of the alpha-2,6-sialyltransferase with its substrate would give a plausible explanation for the preferential sialylation of the branch derived from the alpha-1,3 mannose and the hyposialylation of the alpha-1,6 mannose branch of biantennary *N*-glycans.

The preferential effect on complete sialylation may mean that lobe B of the COG complex is more involved in transport affecting reactions occurring in the late Golgi. The different biochemical phenotypes associated with COG7- and COG8-deficiency could mean that COG subunits differentially affect the trafficking, stability and co-localization of glycosyltransferases and sugar nucleotide transporters.

This paper describes the discovery of the third member of COG-related deficiencies in humans, CDG-IIh or CDG-II/COG8. Serum *N*-glycans from patient cells revealed a unique phenotype mainly consisting of the incomplete addition of one sialic acid molecule to biantennary glycans.The results of glycan analysis of serum or fibroblasts indicate uniquely altered glycosylation, but they cannot reveal the origin of the specific phenotype of this patient. The defects likely result from more than simply a failure to add a portion of the terminal sialic acid. We suggest that measuring the kinetics of BFA-induced Golgi collapse may be a useful screen for COG-deficient patients.

MATERIALS AND METHODS

Materials

All reagents or chemicals were purchased from Sigma unless specified otherwise. Dulbecco's modified eagle medium, penicillin/streptomycin, L-glutamine, Trypsin-EDTA, Lipofectamine 2000, ViraPower™ Lentiviral Directional TOPO® Expression Kit, were from Invitrogen (Carlsbad). Fetal bovine serum was bought from HyClone (Logan). Millex-HV 0.45 μm filter was from Millipore (Billerica, MA). Alexa 488 conjugated Peanut Agglutinin Lectin was purchased from Invitrogen. Polybrene was purchased from Sigma (St. Louis), Polyclonal GPP130 and giantin Alexa-488 (Covance), monoclonal GS15 and GM130 (BD BioSciences), monoclonal Actin (gift of Dr Elena Pasquale), Goat anti-rabbit and Goat anti-mouse HRP (Amersham), UDP-[^{3}H]-Gal American (Radiolabeled Chemicals), CMP-[^{3}H]-sialic acid (Perkin Elmer).

Structural analysis

For permethylation analysis, samples were analyzed as previously described (34,35). Briefly, oligosaccharides were reconstituted in 100 μl dimethylsulfoxide/sodium hydroxide solution and 50 μl of iodomethane was added. After 1 h, an identical amount of these reagents were added and the reaction was allowed to proceed for an additional hour. Equal volumes of chloroform and water were added, the samples vortexed and centrifuged and the aqueous phase removed. This was repeated until the pH of the aqueous phase approached that of the reagent water. Reflectron MALDI-TOF mass spectra were recorded using 2,5-dihydroxybenzoic acid matrix on a Bruker Reflex IV instrument equipped with a nitrogen laser (337 nm, 3 ns peak width) and were collected in triplicate.

CID spectra were collected on an Applied Biosystems API Qstar Pulsar *i* Q-TOF mass spectrometer equipped with an electrospray ion source. Samples were reconstituted at ~2 pmol/μl and analyzed in 30% methanol/0.1% ammonium hydroxide. Approximately 1 pmol of sample was consumed in a typical experiment. The mass spectrometer was operated in the negative ion mode. Standard and sample oligosaccharides were analyzed under identical conditions. Instrument settings were DP −20, FP −220, DP2 −15, CE −40, CAD 4.

To measure the amount and types of *O*-glycans, patient and control cells were incubated for 12 h in 0.25 mM GAP and 10μCi/ml [6-^{3}H]galactose, as previously described (23). The secreted, labeled, GAP-linked glycosides were isolated from the medium and analyzed by amine adsorption HPLC. Identification of glycans was based on comparison with known standards including Core1 and Core2 glycans with polylactosamine repeats. These secreted GAP-linked glycans reflect those made by the intact cells and by non-disrupted Golgi (23).

Biochemical analysis

The analysis of PNGase F-released oligosaccharides by anion exchange chromatography (QAE-Sepahadex) was done as described by Etchison *et al*. (36). Sugar nucleotide uptake assays in SLO-permeabilized fibroblasts and galactosyl- and sialyltransferase assays were performed as described by Wu *et al*. (17). 2-aminobenzamide labelling was done as described

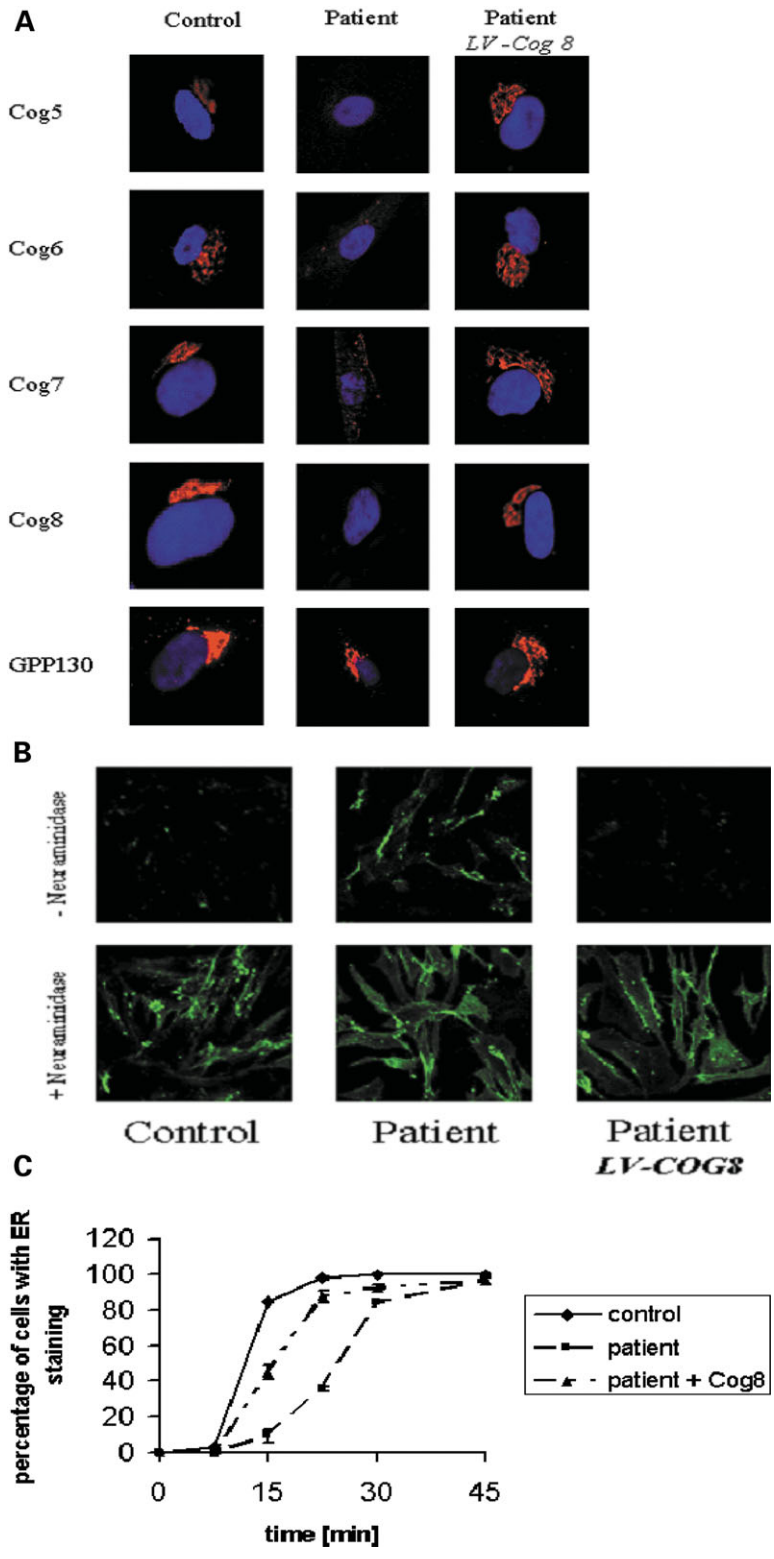

Figure 5. Complementation of patient fibroblasts with wild-type *COG8*. (**A**) Complementation of patient fibroblasts with a lentivirus carrying wild-type *COG8* restored Lobe B Golgi staining comparable with control cells. Cells were also stained with DAPI to show the contrast between Golgi and nuclear staining. The lentivirual construct containing the COG8 gene also had an IRES GFP. (**B**) PNA Alexa-488 staining of control and patient fibroblasts. PNA specifically binds to terminal galactose on *O*-linked glycans. Neuraminidase digestion for 1 h at 37°C removes terminal sialic acid and exposes underlying galactose to PNA binding. Patient cells that have been complemented with the wild-type *COG8* exhibited normal *O*-linked sialylation as shown by decreased PNA staining of patient cells to control level. Because the GFP expression was minimal, we were able to subtract out background levels of GFP. (**C**) BFA-induced retrograde transport kinetics are nearly normalized in *COG8*-complemented fibroblasts.

earlier (30). Western blotting and immunofluorescence were performed as described (18). MALDI-TOF and ESI-MS were done accordingly (29,30). Concanavalin A lectin affinity chromatography has been described before (37).

BFA-induced retrograde transport experiments

Human fibroblasts were cultivated on glass coverslips to 80% confluence. The retrograde transport was induced by replacing the growth media with prewarmed (37°C) medium containing 0.25 μg/ml BFA. The retrograde transport was stopped after 0, 7.5, 15, 22.5, 30 and 45 min by replacing the medium with fixing solution (2% formalin) for 15 min at room temperature. Cells were permeabilized and stained as described (19). The percentage of cells without Golgi staining was determined at the given time points. Between 50 and 100 cells were counted in replicate samples for each time point.

Molecular analysis of the *COG8* gene

Total RNA was prepared from fibroblasts using the Qiagen RNeasy Kit (Qiagen Inc., Valencia, CA, USA) and reverse transcribed using the Super Script first strand cDNA synthesis kit (Invitrogen, Carlsbad, CA).

The complete *COG8* coding region was amplified by using the following primers: COG8-F1: 5′-AAAGTTCGGAG TCAGCGCC-3′ and COG8-R2: 5′-ACCACCTGTTCTCCA TTGGG-3′. Conditions used for the amplification were: 94°C 3 min; (94°C, 1 min; 60°C, 30 s; 72°C, 2 min) 35 times. Final elongation was achieved at 72°C for 10 min.

Genomic DNA was isolated from fibroblast using the Wizard Genomic DNA Purification Kit (Promega, Madison, WI). Primers used span exon3 (COG8-Exon3-F: 5′-GAGA GCATCC TTCCCAGCG-3′ and COG8-Exon3-R: 5′-CCCA TTACCAGAGAAGGCCC-3′) or exon5 (COG8- Exon5-F: 5′- CCTGCCTTAGC CTTCCCAAG-3′ and COG8-Exon5-R: 5′- AGACTGGCAGTGAGCACCG-3′). PCR cycling conditions were: 94°C, 3 min; (94°C, 1 min; 55°C, 30 sec; 72°C, 45 sec) 35 times; 72°C, 10 min.

Lentiviral vectors production and complementation

The COG8 lentiviral vector, LV-hCOG8-IRES2-eGFP, was constructed by replacing the *hALG6* gene in LV-hALG6-IRES2-eGFP with *COG8* cDNA (*SpeI* and *SalI*). LV-GFP was used as a control. Production of the virus was done as described in the Lentiviral Expression System protocol (Invitrogen, Carlsbad, CA). It is important to note that complemented cells expressed minimal background levels of GFP. These background levels were determined from a non Alexa 488 stained sample and were used to subtract the minimal GFP background from subsequent samples.

ACKNOWLEDGEMENTS

We thank Dr Donald Wight for first suggesting CDG analysis of this patient and Dr Monty Krieger for the COG1 and COG2 antibodies. Jesse D. Lyon is acknowledged for his help with some of the experiments. John F. ÓBrien (Mayo Clinic) is acknowledged for ESI-MS analysis. This work was supported by the National Institute of Health (ROI DK55615), and a postdoctoral research fellowship from the Deutsche Forschungsgemeinschaft (KR 2916/1-1) to C.K. and a NIH/NIDDK postdoctoral NRSA fellowship (F32DK072890) to L.S. The BUSM MS Resource is supported by NIH grants P41RR10888 and S1015942.

Conflict of Interest statement. None declared.

REFERENCES

1. Ungar, D., Oka, T., Brittle, E.E., Vasile, E., Lupashin, V.V., Chatterton, J.E., Heuser, J.E., Krieger, M. and Waters, M.G. (2002) Characterization of a mammalian Golgi-localized protein complex, COG, that is required for normal Golgi morphology and function. *J. Cell. Biol.*, **157**, 405–415.
2. Whyte, J.R. and Munro, S. (2001) The Sec34/35 Golgi transport complex is related to the exocyst, defining a family of complexes involved in multiple steps of membrane traffic. *Dev. Cell.*, **1**, 527–537.
3. Ungar, D., Oka, T., Vasile, E., Krieger, M. and Hughson, F.M. (2005) Subunit architecture of the conserved oligomeric Golgi complex. *J. Biol. Chem.*, **280**, 32729–32735.
4. Oka, T., Vasile, E., Penman, M., Novina, C.D., Dykxhoorn, D.M., Ungar, D., Hughson, F.M. and Krieger, M. (2005) Genetic analysis of the subunit organization and function of the conserved oligomeric Golgi (COG) complex: studies of COG5- and COG7-deficient mammalian cells. *J. Biol. Chem.*, **280**, 32736–32745.
5. Ungar, D., Oka, T., Krieger, M. and Hughson, F.M. (2006) Retrograde transport on the COG railway. *Trends Cell. Biol.*, **16**, 113–120.
6. Shestakova, A., Zolov, S. and Lupashin, V. (2006) COG complex-mediated recycling of Golgi glycosyltransferases is essential for normal protein glycosylation. *Traffic*, **7**, 191–204.
7. Zolov, S.N. and Lupashin, V.V. (2005) Cog3p depletion blocks vesicle-mediated Golgi retrograde trafficking in HeLa cells. *J. Cell. Biol.*, **168**, 747–759.
8. Suvorova, E.S., Duden, R. and Lupashin, V.V. (2002) The Sec34/Sec35p complex, a Ypt1p effector required for retrograde intra-Golgi trafficking, interacts with Golgi SNAREs and COPI vesicle coat proteins. *J. Cell. Biol.*, **157**, 631–643.
9. Kingsley, D.M., Kozarsky, K.F., Segal, M. and Krieger, M. (1986) Three types of low density lipoprotein receptor-deficient mutant have pleiotropic defects in the synthesis of N-linked, O-linked, and lipid-linked carbohydrate chains. *J. Cell. Biol.*, **102**, 1576–1585.
10. Kim, D.W., Sacher, M., Scarpa, A., Quinn, A.M. and Ferro-Novick, S. (1999) High-copy suppressor analysis reveals a physical interaction between Sec34p and Sec35p, a protein implicated in vesicle docking. *Mol. Biol. Cell.*, **10**, 3317–3329.
11. Kim, D.W., Massey, T., Sacher, M., Pypaert, M. and Ferro-Novick, S. (2001) Sgf1p, a new component of the Sec34p/Sec35p complex. *Traffic*, **2**, 820–830.
12. Ram, R.J., Li, B. and Kaiser, C.A. (2002) Identification of Sec36p, Sec37p, and Sec38p: components of yeast complex that contains Sec34p and Sec35p. *Mol. Biol. Cell.*, **13**, 1484–1500.
13. VanRheenen, S.M., Cao, X., Lupashin, V.V., Barlowe, C. and Waters, M.G. (1998) Sec35p, a novel peripheral membrane protein, is required for ER to Golgi vesicle docking. *J. Cell. Biol.*, **141**, 1107–1119.
14. VanRheenen, S.M., Cao, X., Sapperstein, S.K., Chiang, E.C., Lupashin, V.V., Barlowe, C. and Waters, M.G. (1999) Sec34p, a protein required for vesicle tethering to the yeast Golgi apparatus, is in a complex with Sec35p. *J. Cell. Biol.*, **147**, 729–742.
15. Farkas, R.M., Giansanti, M.G., Gatti, M. and Fuller, M.T. (2003) The *Drosophila* Cog5 homologue is required for cytokinesis, cell elongation, and assembly of specialized Golgi architecture during spermatogenesis. *Mol. Biol. Cell.*, **14**, 190–200.
16. Kubota, Y., Sano, M., Goda, S., Suzuki, N. and Nishiwaki, K. (2006) The conserved oligomeric Golgi complex acts in organ morphogenesis via glycosylation of an ADAM protease in *C. elegans*. *Development*, **133**, 263–273.
17. Wu, X., Steet, R.A., Bohorov, O., Bakker, J., Newell, J., Krieger, M., Spaapen, L., Kornfeld, S. and Freeze, H.H. (2004) Mutation of the COG complex subunit gene COG7 causes a lethal congenital disorder. *Nat. Med.*, **10**, 518–523.

18. Foulquier, F., Vasile, E., Schollen, E., Callewaert, N., Raemaekers, T., Quelhas, D., Jaeken, J., Mills, P., Winchester, B., Krieger, M. *et al*. (2006) Conserved oligomeric Golgi complex subunit 1 deficiency reveals a previously uncharacterized congenital disorder of glycosylation type II. *Proc. Natl. Acad. Sci. USA*, **103**, 3764–3769.
19. Steet, R. and Kornfeld, S. (2006) COG-7-deficient human fibroblasts exhibit altered recycling of golgi proteins. *Mo.l Biol. Cell.*, **17**, 2312–2321.
20. Freeze, H.H. (2006) Genetic defects in the human glycome. *Nat. Rev. Genet.*, **7**, 537–551.
21. Marquardt, T. and Denecke, J. (2003) Congenital disorders of glycosylation: review of their molecular bases, clinical presentations and specific therapies. *Eur. J. Pediatr.*, **162**, 359–379.
22. Chacko, B.K. and Appukuttan, P.S. (2001) Peanut (*Arachis hypogaea*) lectin recognizes alpha-linked galactose, but not N-acetyl lactosamine in N-linked oligosaccharide terminals. *Int. J. Biol. Macromol.*, **28**, 365–371.
23. Kim, S., Miura, Y., Etchison, J.R. and Freeze, H.H. (2001) Intact Golgi synthesize complex branched O-linked chains on glycoside primers: Evidence for the functional continuity of seven glycosyltransferases and three sugar nucleotide transporters. *Glycoconj. J.*, **18**, 623–633.
24. Oka, T., Ungar, D., Hughson, F.M. and Krieger, M. (2004) The COG and COPI complexes interact to control the abundance of GEARs, a subset of Golgi integral membrane proteins. *Mol. Biol. Cell.*, **15**, 2423–2435.
25. Doms, R.W., Russ, G. and Yewdell, J.W. (1989) Brefeldin A redistributes resident and itinerant Golgi proteins to the endoplasmic reticulum. *J. Cell. Biol.*, **109**, 61–72.
26. Donaldson, J.G., Kahn, R.A., Lippincott-Schwartz, J. and Klausner, R.D. (1991) Binding of ARF and beta-COP to Golgi membranes: possible regulation by a trimeric G protein. *Science*, **254**, 1197–1199.
27. Fotso, P., Koryakina, Y., Pavliv, O., Tsiomenko, A.B. and Lupashin, V.V. (2005) Cog1p plays a central role in the organization of the yeast conserved oligomeric Golgi complex. *J. Biol. Chem.*, **280**, 27613–27623.
28. Wopereis, S., Morava, E., Grunewald, S., Mills, P.B., Winchester, B.G., Clayton, P., Coucke, P., Huijben, K.M. and Wevers, R.A. (2005) A combined defect in the biosynthesis of N- and O-glycans in patients with cutis laxa and neurological involvement: the biochemical characteristics. *Biochim. Biophys. Acta*, **1741**, 156–164.
29. Mandato, C., Brive, L., Miura, Y., Davis, J.A., Di Cosmo, N., Lucariello, S., Pagliardini, S., Seo, N.S., Parenti, G., Vecchione, R. *et al*. (2006) Cryptogenic liver disease in four children: a novel congenital disorder of glycosylation. *Pediatr. Res.*, **59**, 293–298.
30. Miura, Y., Tay, S.K., Aw, M.M., Eklund, E.A. and Freeze, H.H. (2005) Clinical and biochemical characterization of a patient with congenital disorder of glycosylation (CDG) IIx. *J. Pediatr.*, **147**, 851–853.
31. van den Eijnden, D.H., Joziasse, D.H., Dorland, L., van Halbeek, H., Vliegenthart, J.F. and Schmid, K. (1980) Specificity in the enzymic transfer of sialic acid to the oligosaccharide branches of b1- and triantennary glycopeptides of alpha 1-acid glycoprotein. *Biochem. Biophys. Res. Commun.*, **92**, 839–845.
32. Joziasse, D.H., Schiphorst, W.E., van den Eijnden, D.H., van Kuik, J.A., van Halbeek, H. and Vliegenthart, J.F. (1985) Branch specificity of bovine colostrum CMP-sialic acid: N-acetyllactosaminide alpha 2-6-sialyltransferase. Interaction with biantennary oligosaccharides and glycopeptides of N-glycosylproteins. *J. Biol. Chem.*, **260**, 714–719.
33. Joziasse, D.H., Schiphorst, W.E., Van den Eijnden, D.H., Van Kuik, J.A., Van Halbeek, H. and Vliegenthart, J.F. (1987) Branch specificity of bovine colostrum CMP-sialic acid: Gal beta 1-4GlcNAc-R alpha 2-6-sialyltransferase. Sialylation of bi-, tri-, and tetraantennary oligosaccharides and glycopeptides of the N-acetyllactosamine type. *J. Biol. Chem.*, **262**, 2025–2033.
34. Ciucanu, I. and Kerek, F. (1984) A simple and rapid method for the permethylation of carbohydrates. *Carbohydr. Res.*, **131**, 209–217.
35. Cipollo, J.F., Awad, A.M., Costello, C.E. and Hirschberg, C.B. (2004) srf-3, a mutant of Caenorhabditis elegans, resistant to bacterial infection and to biofilm binding, is deficient in glycoconjugates. *J. Biol. Chem.*, **279**, 52893–52903.
36. Etchison, J.R., Srikrishna, G. and Freeze, H.H. (1995) A novel method to co-localize glycosaminoglycan-core oligosaccharide glycosyltransferases in rat liver Golgi. Co-localization of galactosyltransferase I with a sialyltransferase. *J. Biol. Chem.*, **270**, 756–764.
37. Srikrishna, G., Brive, L. and Freeze, H.H. (2005) Novel carboxylated N-glycans contain oligosaccharide-linked glutamic acid. *Biochem. Biophys. Res. Commun.*, **332**, 1020–1027.